Hideki Kikumoto

Variations in the power-law index with stability and height for wind profiles in the urban boundary layer

Hideki Kikumoto[1], Ryozo Ooka[2], Hirofumi Sugawara[3]

[1] *Institute of Industrial Science, The University of Tokyo, Tokyo, Japan, kkmt@iis.u-tokyo.ac.jp*

[2] *Institute of Industrial Science, The University of Tokyo, Tokyo, Japan, ooka@iis.u-tokyo.ac.jp*

[3] *Earth and Ocean Sciences, National Defense Academy of Japan, Kanagawa, Japan, hiros@nda.ac.jp*

Dated: June 15, 2015

1. Introduction

Among the various methods to express the relationship between wind velocity and height above ground (z), the power-law (PL) is one of the most common in engineering. Although its theoretical basis is not as clear as the logarithmic-law, past observations have shown its potential in modeling wind profiles in the atmospheric boundary layers (Counihan, 1975; Tamura et al., 2007).

The PL was originally proposed for wind profiles of extremely high velocity in structural engineering (Davenport, 1960), so that high velocity and neutrality were prerequisites for its use. However, because of its simple mathematical expression, it has also been applied in other contexts, such as wind environment and air pollution (Tominaga et al., 2008). In such cases, the neutrality of the boundary layer is not assured and the accuracy of the PL can change with the stability. Previous studies have also reported the dependence of the power-law index (PLI) on the stability and height at which the PL is evaluated (Irwin, 1979; Hanafusa, 1986).

In this research, wind profiles were measured in an urban boundary layer to investigate the variations of the PLI with velocity, stability, and height above ground. A Doppler lidar system (DLS) was used simultaneously with an ultrasonic anemometer (UA). Vertical profiles of the wind velocity were measured by the DLS and the velocities and turbulent fluxes of momentum and heat were corrected by the eddy covariance method (ECM) using the UA.

2. Observation site and instrumentation

The DLS was installed on a building rooftop at the Institute of Industrial Science (University of Tokyo, Meguro-ku, Tokyo, Japan). Velocities were measured between 67.5 and 527.5 m high for every 20 m (24 levels). The UA was set on a tower at the Tokai University campus (Shibuya-ku, Tokyo, Japan), at a ground height of 52 m. The distance between the sites was about 600 m (Fig. 1), with no undulating terrain between them, and their altitude difference was 2 m.

Observations were recorded for seven months in September–December 2013 and April–June 2014. Although the temporal resolution of the DLS data was of about 30 s, 10 min averages were used. For the ECM data, the discussions were based on 30 min averages.

Since the DLS is based on remote sensing using atmospheric aerosols, it sometimes fails to obtain data in unfavorable atmospheric conditions. To keep the high quality of the data, we only used profiles for which velocities could be measured for all observation heights. Consequently, during the observation period, the data acquisition percentage of the 10 min averaged profiles was 58.9%.

Fig. 1 Aerial photo map of the observation site (Tokyo, Japan; from Google maps)

3. Observed data

3.1 Wind velocity

Figure 2 shows the frequency distributions of the horizontal wind velocity (u_b) for the lowest DLS level and for the ECM. The mean u_b for the 10 min average was 4.3 m/s, with 60% of the velocities <5 m/s. Even though there was a 16 m difference in the measuring height between the DLS and the ECM, their frequency distribution shape was very similar. Therefore, the two measuring sites were assumed to reflect the same wind environment, regardless of their distance.

Figure 3 compares the velocities of the west and south wind components measured by the DLS and ECM. Since their correlation was very high, we considered valid the asumption that the DLS and ECM data were measured at the same location.

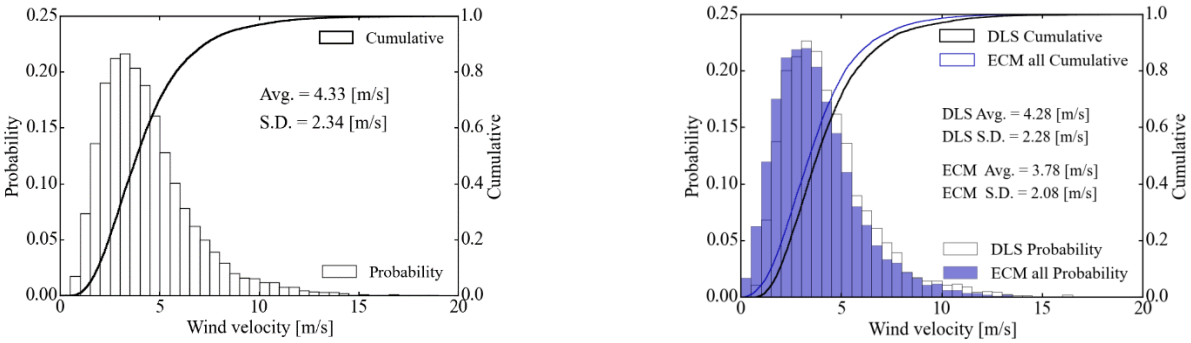

Fig. 2 Probability and cumulative density functions of the horizontal wind velocity measured by the Doppler lidar system (DLS, 67.5 m high) and eddy covariance method (ECM) for the (i) 10 min average and (ii) 30 min average

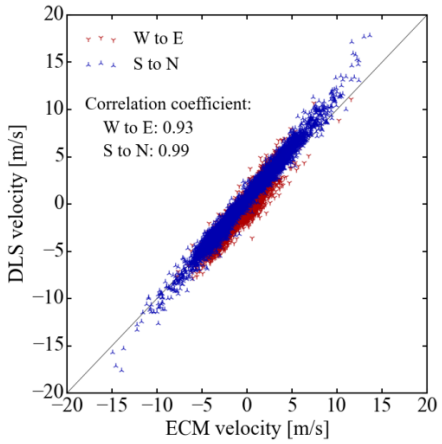

Fig. 3 Correlation of the wind velocities from the eddy covariance method (ECM, 52 m high) and Doppler lidar system (DLS, 67.5 m high). The west and south wind components for the 30 min average are compared between the observations

3.2 Variations in wind direction

The frequency distributions of the wind direction measured by the DLS at 67.5 and 467.5 m high are shown in Fig. 4. The results include the distributions for all velocities and high velocities (u_b > 6 m/s). During the observations, south and north wind was the most common. However, the distribution was slightly different for the different heights, with the peaks observed for 0 and 60° at 67.5 m not clear at 467.5 m. However, this difference became small for higher velocities.

Figure 5 shows the scatter plots between the wind velocity and the deviation in wind direction in relation to the direction measured at the lowest DLS level (wd_b) for four observation heights. Even though the deviation tended to increase with the increase in height difference, it decreased with the increase in wind velocity for all heights. For wind velocities below about 5 m/s, the deviation was very large, e.g., about 180° for a 100 m height difference for very low velocities. For these cases, the determination of the prevailing wind direction was very difficult.

Figure 6 shows the vertical profiles of the mean and standard deviations of the wind direction deviation based on the wind velocity and direction at z = 67.5 m. As shown in Fig. 5, the wind direction deviation became very large when all wind velocities were included. When using high wind velocity data, the mean deviation became small, i.e., 7° at the highest observation point. The mean deviation tended to become positive with the increase in observation height, which agrees with the Ekman spiral predictions.

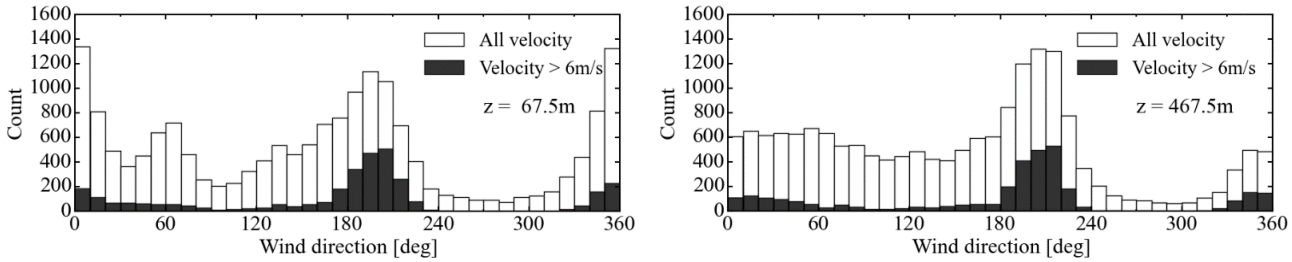

Fig. 4 Frequency distributions of the wind direction for the 10 min average measured by the Doppler lidar system (DLS) at heights of 67.5 and 467.5 m. The high velocity data were extracted using the horizontal wind velocity for the lowest DLS level (u_b)

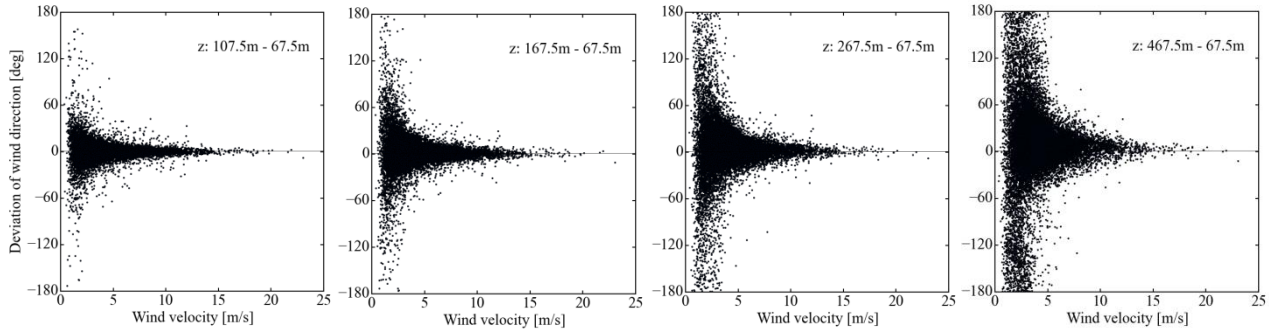

Fig. 5 Relationship between the wind velocity and deviation in the wind direction for z = 107.5, 167.5, 267.5, and 467.5 m based on the wind velocity (u_b) and direction (wd_b) at a height of 67.5 m (10 min average)

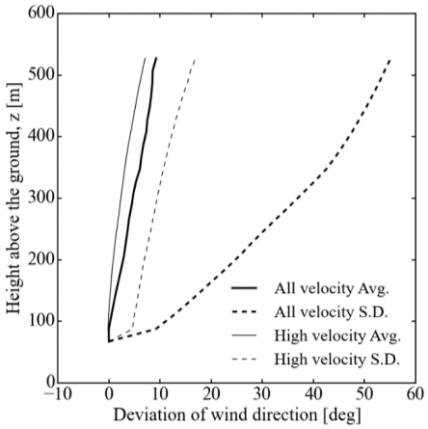

Fig. 6 Vertical profiles of the average (Avg.) and standard deviation (S.D.) of the wind direction deviation in relation to the direction at a height of 67.5 m. The high velocity data corresponds to wind velocities (u_b) ≥ 6 m/s

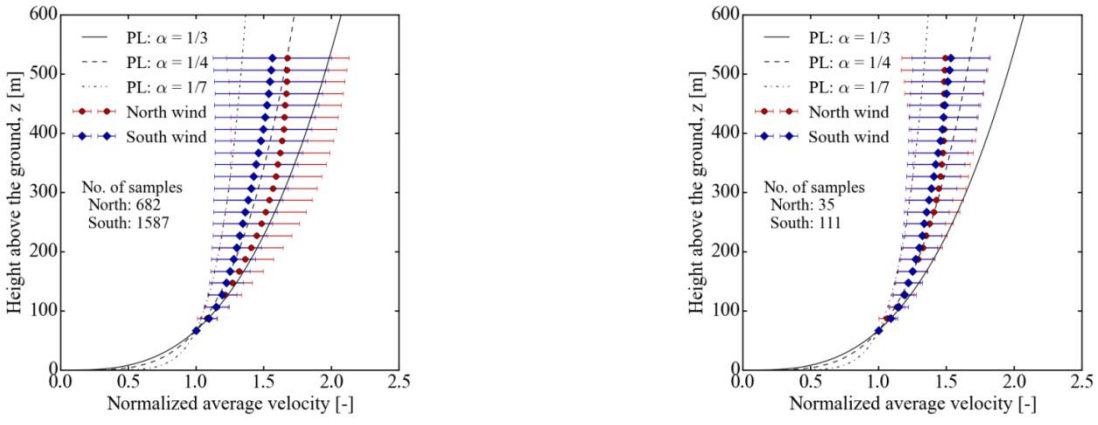

Fig. 7 Ensemble-averaged profiles of the wind velocity (u_b) based on the 10 min average for (i) u_b ≥ 6 m/s and (ii) u_b ≥ 12 m/s. Each profile is averaged after normalization using the horizontal wind velocity for the lowest Doppler lidar system (DLS) level (u_b). The error bars show the standard deviation of the profiles. North wind corresponds to 0 ≤ wind direction (wd_b) < 20° or 340 ≤ wd_b < 360°, while south wind corresponds to 180 ≤ wd_b < 220°

3.3 Power-law index of the average wind profiles

Figure 7 presents the mean profiles of the (high) wind velocities obtained by the ensemble averages of the 10 min average profiles measured by the DLS. North and south wind was found at z = 67.5 m and averaged for each wind direction. Although the variation of the wind profiles for the 10 min average remained relatively large for wind velocities >6 m/s, the mean velocity could be fitted using the PL, with a PLI of 1/3 and 1/4 for north and south wind, respectively, below 200 m high. When using data for wind velocities >12 m/s to calculate the average, the PLI difference depending on the wind direction decreased, with a PLI of 1/4 allowing a good prediction of both north and south wind profiles. Regardless of its value, the wind velocity tended to move away from the wind profile based on the PL using a unique PLI, meaning that the PLI could change according to the height used for the estimation.

3.4 Wind velocity and power-law index

When a wind profile obeys the PL, its PLI (α) can be evaluated by the following equation:

$$\alpha = \frac{\ln(u_2/u_1)}{\ln(z_2/z_1)} \quad (1)$$

where u_i is the wind velocity (m/s) at height z_i (i = 1, 2, in m).

Figure 8 shows the relationship between the wind velocity and the PLI from the 30 min averaged velocities setting z_1 and z_2 in (1) to 67.5 and 167.5 m, respectively. Figure 9 presents the frequency distributions of the PLI derived as for Fig. 8. With the decrease in wind velocity, the PLI exhibited a larger variety, sometimes reaching negative values. However, for high wind velocities, the PLI converged to around 1/4, as in Fig. 7. Although there was a large variation in the PLI, it tended to be smaller for low velocities. The mode of the PLI for all velocities was about 0.15, with the distribution shape having a long tail towards a larger PLI.

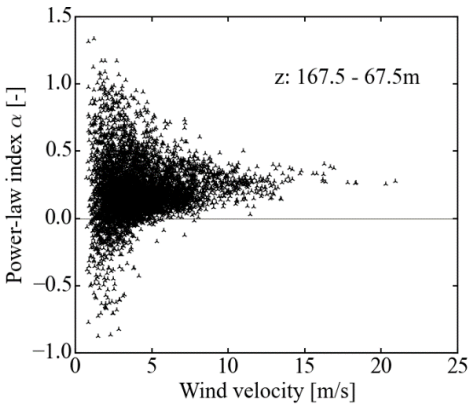

Fig. 8 Wind velocity (u_b) and power-law index (PLI, α) derived from the 30 min average of the wind velocity at 67.5 and 167.5 m high

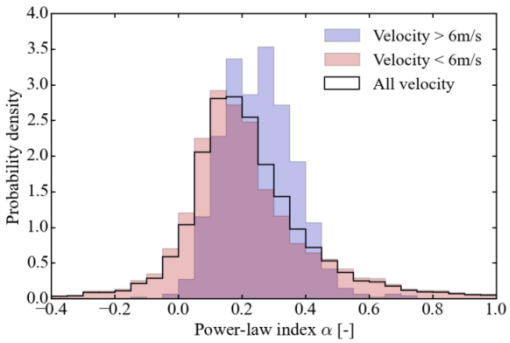

Fig. 9 Probability density functions of the power-law index (PLI) derived from the 30 min wind velocity average at 67.5 and 167.5 m high. The data are divided in high and low velocity

3.5 Atmospheric stability and power-law index

Previous studies showed that the PLI depended not only on the roughness of the land surface, but also on the atmospheric stability (Touma, 1977; Irwin, 1979; Hanafusa et al., 1986), as explained using atmospheric stability

parameters, such as the Pasquill stability class and the Monin-Obukhov length L (Monin and Obukhov, 1954). In this study, we used L as a stability parameter derived from the fluxes of momentum and heat from the ECM.

Figure 10 shows the scatter plots between the 1/L and the PLI. To know the influence of the height, the PLI was calculated using two different heights. When 1/L was nearly zero (neutral), the PLI was 0.2–0.3, in accordance with the fact that 1/4 is one of the PLI standard values for airflow analysis in urban areas. The PLI became small for unstable atmospheric conditions (negative 1/L) and large for stable conditions (positive 1/L). However, it remained around 0.1 until a certain level of instability was reached. The height difference when deriving the PLI did not result in large differences in the PLI trends.

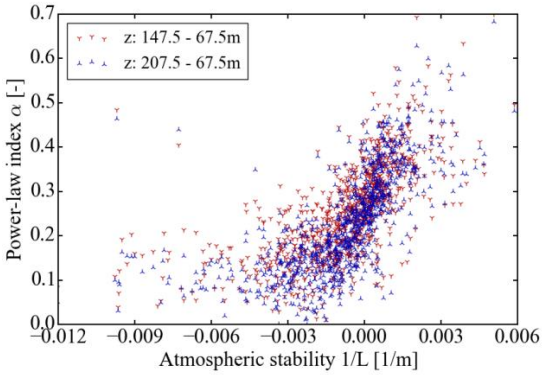

Fig. 10 Relationship between the atmospheric stability (1/L) and the power-law index (PLI). The Monin-Obukhov length L was calculated using statistics from the eddy covariance method (ECM). The PLI was determined from 30 min wind velocity average for heights of 67.5 and 147.5 or 207.5 m. Data for wind velocities (u_b) ≥ 6 m/s were used

4. Conclusions

A Doppler lidar system and an ultrasonic anemometer were simultaneously installed to measure wind profiles and the atmospheric stability in the urban boundary layer of Tokyo, Japan. The 10 min wind velocity averages were <5 m/s at 67.5 m high during 60% of the observation period. For low wind velocities, the differences in wind direction with height were very large, difficulting the determination of the prevailing wind direction. The power-law could be used to model the mean wind profiles for high wind velocities (u_b > 6 m/s) and for the lower urban boundary layer (z < 200 m). For wind profiles of high velocity, the power-law index converged to 1/4 (0.25) and the effect of the atmospheric stability on the power-law index could be connected with the inverse of the Monin-Obukhov length. Although the power-law index was smaller (~0.15), on average, for profiles of low or all wind velocities, its large variability resulted in a difficult definition of a representative power-law index or application of the power-law to the wind profiles.

The analysis of thermal and air pollution in urban areas is more relevant for low wind velocities, since that results in more serious events that cover a larger fraction of people's daily lives. This study revealed the difficulty in modeling wind profiles for low velocities, which should be addressed in future work.

Acknowledgments

This work was partly supported by the Japan Society for the Promotion of Science (JSPS) KAKENHI Grants No. 24226013, 26709041, and 24241008.

References

Counihan J., 1975: Adiabatic atmospheric boundary layers: A review and analysis of data from the period 1880–1972. *Atmospheric Environment*, **9**, 871–905

Davenport A.G., 1960: Rationale for determining design wind velocities. *Journal of the Structural Division*, **86**, 39–68

Hanafusa T. et al., 1986. Dependence of the exponent in power law wind profiles on stability and height interval. *Atmospheric Environment*, **20**, 2059–2066.

Irwin J.S., 1979: A theoretical variation of the wind profile power-law exponent as a function of surface roughness and stability. *Atmospheric Environment*, **13**, 191–194

Monin A.S., Obukhov A.M., 1954: Basic laws of turbulent mixing in the surface layer of the atmosphere. *Tr. Akad. Nauk SSSR Geophiz. Inst.*, **24**, 163–187

Tamura Y. et al., 2007: Profiles of mean wind speeds and vertical turbulence intensities measured at seashore and two inland sites using Doppler sodars. *Journal of Wind Engineering and Industrial Aerodynamics*, **95**, 411–427

Tominaga Y. et al., 2008: AIJ guidelines for practical applications of CFD to pedestrian wind environment around buildings. *Journal of Wind Engineering and Industrial Aerodynamics*, **96**, 1749–1761

Touma J.S., 1977: Dependence of the wind profile power law on stability for various locations. *Journal of the Air Pollution Control Association*, **27**, 863–866